JACS
JOURNAL OF THE AMERICAN CHEMICAL SOCIETY

ARTICLE

pubs.acs.org/JACS

# Comprehensive Thermochemistry of W−H Bonding in the Metal Hydrides $CpW(CO)_2(IMes)H$, $[CpW(CO)_2(IMes)H]^{\bullet+}$, and $[CpW(CO)_2(IMes)(H)_2]^+$. Influence of an *N*-Heterocyclic Carbene Ligand on Metal Hydride Bond Energies

John A. S. Roberts, Aaron M. Appel, Daniel L. DuBois, and R. Morris Bullock*

Chemical and Materials Sciences Division, Pacific Northwest National Laboratory, P.O. Box 999, K2-57, Richland, Washington 99352, United States

Supporting Information

**ABSTRACT:** The free energies interconnecting nine tungsten complexes have been determined from chemical equilibria and electrochemical data in MeCN solution ($T$ = 22 °C). Homolytic W−H bond dissociation free energies are 59.3(3) kcal mol$^{-1}$ for $CpW(CO)_2(IMes)H$ and 59(1) kcal mol$^{-1}$ for the dihydride $[CpW(CO)_2(IMes)(H)_2]^+$ (where IMes = 1,3-bis(2,4,6-trimethylphenyl)imidazol-2-ylidene), indicating that the bonds are the same within experimental uncertainty for the neutral hydride and the cationic dihydride. For the radical cation, $[CpW(CO)_2(IMes)H]^{\bullet+}$, W−H bond homolysis to generate the 16-electron cation $[CpW(CO)_2(IMes)]^+$ is followed by MeCN uptake, with free energies for these steps being 51(1) and −16.9(5) kcal mol$^{-1}$, respectively. Based on these two steps, the free energy change for the net conversion of $[CpW(CO)_2(IMes)H]^{\bullet+}$ to $[CpW(CO)_2(IMes)(MeCN)]^+$ in MeCN is 34(1) kcal mol$^{-1}$, indicating a much lower bond strength for the 17-electron radical cation of the metal hydride compared to the 18-electron hydride or dihydride. The p$K_a$ of $CpW(CO)_2(IMes)H$ in MeCN was determined to be 31.9(1), significantly higher than the 26.6 reported for the related phosphine complex, $CpW(CO)_2(PMe_3)H$. This difference is attributed to the electron donor strength of IMes greatly exceeding that of $PMe_3$. The p$K_a$ values for $[CpW(CO)_2(IMes)H]^{\bullet+}$ and $[CpW(CO)_2(IMes)(H)_2]^+$ were determined to be 6.3(5) and 6.3(8), much closer to the p$K_a$ values reported for the $PMe_3$ analogues. The free energy of hydride abstraction from $CpW(CO)_2(IMes)H$ is 74(1) kcal mol$^{-1}$, and the resultant $[CpW(CO)_2(IMes)]^+$ cation is significantly stabilized by binding MeCN to form $[CpW(CO)_2(IMes)(MeCN)]^+$, giving an effective hydride donor ability of 57(1) kcal mol$^{-1}$ in MeCN. Electrochemical oxidation of $[CpW(CO)_2(IMes)]^-$ is fully reversible at all observed scan rates in cyclic voltammetry experiments ($E°$ = −1.65 V vs $Cp_2Fe^{+/0}$ in MeCN), whereas $CpW(CO)_2(IMes)H$ is reversibly oxidized ($E°$ = −0.13(3) V) only at high scan rates (800 V s$^{-1}$). For $[CpW(CO)_2(IMes)(MeCN)]^+$, high-pressure NMR experiments provide an estimate of $\Delta G°$ = 10.3(4) kcal mol$^{-1}$ for the displacement of MeCN by $H_2$ to give $[CpW(CO)_2(IMes)(H)_2]^+$.

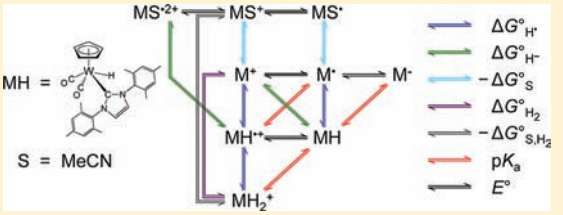


## INTRODUCTION

Transition metal hydrides play a pivotal role in organometallic chemistry and catalysis, mediating the formation of bonds to hydrogen, including C−H, O−H, and H−H bonds. The versatility of reactions exhibited by metal hydrides is documented by the cleavage of the M−H bond in stoichiometric and catalytic reactions as a proton,[1] a hydrogen atom,[2] or a hydride[3] (Scheme 1). A better understanding of the factors that influence the thermodynamics of cleavage of M−H bonds can help in the design and discovery of new stoichiometric, catalytic, and electrocatalytic[4] reactions. Based on M−H acidities, homolytic M−H bond dissociation free energies (BDFEs), and hydride donor abilities, comprehensive free energy analyses have been conducted for a variety of late transition metal hydride systems based on Co,[5] Rh,[6] Ni,[7−9] Pd,[10,11] and Pt,[7] and for S−H bonding in systems containing a $Cp^*_2Mo_2S_4$ core.[12,13] Homolytic and heterolytic M−H bond dissociation enthalpy values have been reported for some Cr, Mo, and W hydrides bearing single Cp- or Tp-derived (Tp = hydridotris(pyrazolyl)borate) ligands.[14−20]

The electronic and steric influences of phosphine ligands have been studied in detail for decades, following landmark studies by Tolman.[21] Extensive studies have determined how phosphine ligands influence the key thermochemical properties of metal hydrides, including p$K_a$ values,[1,22−24] homolytic bond dissociation energies

**Scheme 1**

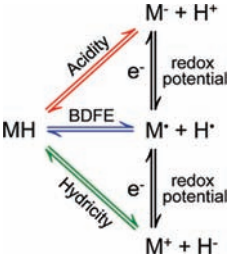


**Received:** April 8, 2011
**Published:** July 22, 2011

  

(BDEs),[17,19,20,25−27] and hydride donor abilities.[5−8,11,14,28,29] In contrast, quantitative data revealing how *N*-heterocyclic carbene (NHC) ligands[30] influence these same properties of metal hydride complexes are comparatively sparse. Nolan and co-workers reported systematic studies that evaluated the steric and electronic properties of NHC ligands.[31] In general, it was found that NHC ligands are more strongly donating than tertiary phosphines[31] and that, compared to phosphine substituent electronic effects, there is not a large difference in electronic properties among NHC ligands having different *N*,*N*′ substituents. Recent calculations by Gusev have provided comparisons of the electronic and steric properties of NHC ligands.[32] Burgess and co-workers reported calculations showing that Ir(V) hydrides with NHC ligands can be significantly less acidic than related metal hydrides with phosphine ligands.[33]

We report here a comprehensive study of the thermochemistry of the W−H bond of the metal hydride $CpW(CO)_2(IMes)H$,[34,35] the radical cation $[CpW(CO)_2(IMes)H]^{\bullet+}$, and the dihydride $[CpW(CO)_2(IMes)(H)_2]^+$ (where IMes = 1,3-bis(2,4,6-trimethylphenyl)imidazol-2-ylidene, a prototypical NHC ligand). The thermochemical cycles employed here map the free energy changes for transformations among $CpW(CO)_2(IMes)H$ and species related to it by transfer of electrons, $H^+$, $H^\bullet$, $H^-$, $H_2$, and MeCN. Our results reveal a system having a substantial range of homolytic and heterolytic BDFEs, with acidities spanning 25.6 p$K_a$ units (~35 kcal mol$^{-1}$) and with homolytic BDFEs spanning 25 kcal mol$^{-1}$. These values are significantly influenced by the exergonic solvation of the 16-electron cation $[CpW(CO)_2(IMes)]^+$ by MeCN to give $[CpW(CO)_2(IMes)(MeCN)]^+$. We first present the results of chemical equilibrium determinations, including proton transfer from $CpW(CO)_2(IMes)H$ and the displacement of MeCN by $H_2$ at $[CpW(CO)_2(IMes)(MeCN)]^+B(C_6F_5)_4^-$, and give a brief discussion of the oxidation electrochemistry of both $CpW(CO)_2(IMes)H$ and $[CpW(CO)_2(IMes)]^-[K(18\text{-crown-6})]^+$. We then use these results to develop the free energy diagram, drawing comparisons with related systems $CpW(CO)_2LH$ (L = CO, $PMe_3$).

## RESULTS

**Determination of the Acidity (p$K_a$) of $CpW(CO)_2(IMes)H$.** The p$K_a$ of $CpW(CO)_2(IMes)H$ in MeCN was determined using $^1$H NMR to measure the equilibrium constant for deprotonation of the hydride by the trimethyl variant of Verkade's superbase[36] (abbreviated as VSB; see eq 1; p$K_a^{MeCN}$ = 32.90 for $[(VSB)H]^+$).[37]

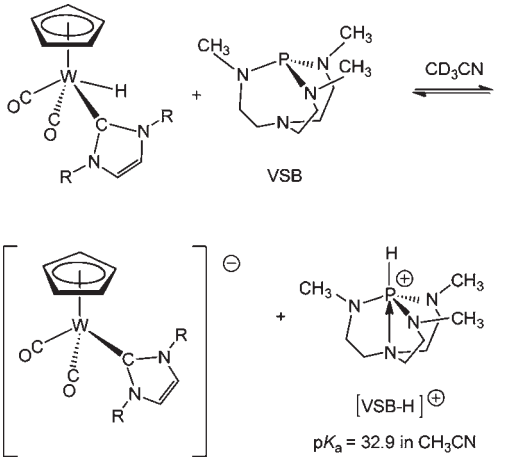


(1)

To verify that equilibrium had been established, both the forward and reverse reactions were carried out. For the reverse reaction, the conjugate base of $CpW(CO)_2(IMes)H$ was prepared by deprotonation with KH in the presence of 18-crown-6 to afford the metal anion $[CpW(CO)_2(IMes)]^-[K(18\text{-crown-6})]^+$, which has been characterized by spectroscopic data as well as by crystallography.[38] These measurements gave $K_{eq}$ = 0.10(2), leading to a value of p$K_a^{MeCN}$ = 31.9(1) for $CpW(CO)_2(IMes)H$ (uncertainty is given at the 2$\sigma$ confidence level).

**High-Pressure NMR Spectroscopic Studies: Formation of $[CpW(CO)_2(IMes)(H)_2]^+B(C_6F_5)_4^-$ in THF-$d_8$ under Hydrogen and Determination of $K_{THF,H_2}$.** The equilibrium for displacement of THF-$d_8$ by $H_2$ in $[CpW(CO)_2(IMes)(THF\text{-}d_8)]^+$ (eq 2) was observed using THF-$d_8$ as solvent at elevated $H_2$ pressures, allowing determination of $K_{THF,H_2}$.[35]

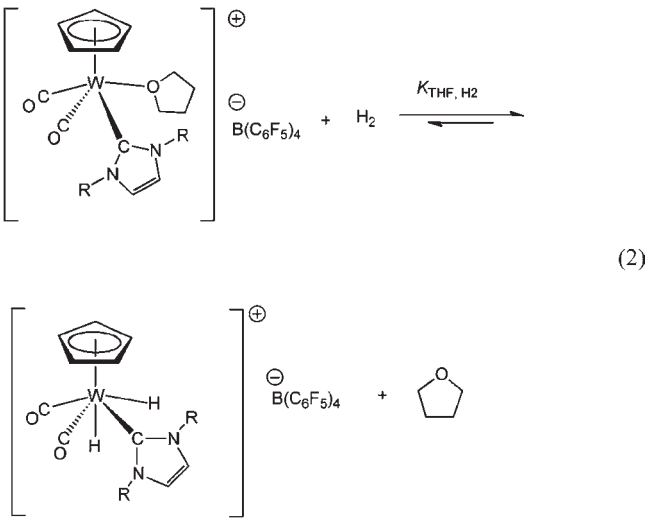


(2)

This equilibrium was studied by NMR spectroscopy using heavy-walled polyether ether ketone (PEEK) NMR tubes.[39] Using this method, solution $H_2$ concentrations may be varied systematically using a single sample and may be raised and lowered as needed in order to approach equilibrium from the product or reactant side. $H_2$ concentrations exceeding 300 mM were achieved at $P_{H_2}$ = 170 atm (20 °C), compared to concentrations of about 9 mM obtained with $P_{H_2}$ = 4 atm at room temperature.[34,35] Distinct Cp resonances were observed for the THF-$d_8$ adduct and the dihydride, indicating slow chemical exchange on the NMR time scale. These resonances were partially overlapping and were integrated using digital line shape analysis. Measurements taken with $P_{H_2}$ = 3.4 atm, 6.8 atm, and again at 3.4 atm (in that order), established $K_{THF,H_2}$ = 0.5(3) atm$^{-1}$ in neat THF-$d_8$, in good agreement with an earlier measurement at a single pressure.[35]

**Determination of $K_{MeCN,H_2}$.** For $[CpW(CO)_2(IMes)(CD_3CN)]^+$, displacement of $CD_3CN$ by $H_2$ was not observed in $CD_3CN$, even at $H_2$ pressures exceeding 200 atm. However, using THF-$d_8$ as solvent, displacement of the coordinated MeCN by $H_2$ was observed, allowing determination of $K_{MeCN,H_2}$ (eq 3).

$$[CpW(CO)_2(IMes)(MeCN)]^+ + H_2 \overset{K_{MeCN,H_2}}{\rightleftharpoons} [CpW(CO)_2(IMes)(H)_2]^+ + MeCN \quad (3)$$


dx.doi.org/10.1021/ja202830w |J. Am. Chem. Soc. 2011, 133, 14604–14613

When $[CpW(CO)_2(IMes)(MeCN)]^+B(C_6F_5)_4^-$ was dissolved in THF-$d_8$ without added $H_2$, both $[CpW(CO)_2(IMes)(MeCN)]^+$ and trace amounts (<1%) of $[CpW(CO)_2(IMes)(THF\text{-}d_8)]^+$ were observed, along with free MeCN. With $P_{H_2}$ = 34, 170, and 136 atm, $[CpW(CO)_2(IMes)(H)_2]^+$ was also observed along with free $H_2$. In these spectra, $[CpW(CO)_2(IMes)(H)_2]^+$ was observed as 3−15% of the total cationic tungsten material, corresponding to $K_{MeCN,H_2} = 3(2) \times 10^{-8}$ atm$^{-1}$ ($\Delta G^\circ$ = 10.3(3) kcal mol$^{-1}$; eq 3) with neat MeCN taken as its standard state (equivalent to $K_{MeCN,H_2} = 5(2) \times 10^{-4}$ when $[H_2]$ = 1 M and [MeCN] = 1 M are taken as their standard states; see the Supporting Information.) The equilibrium constant $K_{MeCN,H_2}$ for displacement of MeCN by $H_2$ at $[CpW(CO)_2(IMes)(MeCN)]^+$ (eq 3) is used in the determination of the homolytic W−H BDFE and $pK_a^{MeCN}$ of $[CpW(CO)_2(IMes)(H)_2]^+$, as discussed below.

**Electrochemistry of $[CpW(CO)_2(IMes)]^-[K(18\text{-crown-6})]^+$.** The anion $[CpW(CO)_2(IMes)]^-$ exhibits a reversible one-electron oxidation, producing the 17-electron metal radical $CpW(CO)_2(IMes)^\bullet$. Subsequent irreversible oxidation of $CpW(CO)_2(IMes)^\bullet$ affords the cationic solvent adduct $[CpW(CO)_2(IMes)(MeCN)]^+$. The cyclic voltammogram of $[CpW(CO)_2(IMes)]^-[K(18\text{-crown-6})]^+$ recorded in MeCN (0.2 M $^nBu_4N^+PF_6^-$; 0.1 V s$^{-1}$) is shown in Figure 1. Redox potentials are presented in Table 1. Cyclic voltammograms collected at a range of different scan rates and analyte concentrations have been digitally simulated using a model that includes this solvent binding reaction,[40] affording estimates of $E^\circ$ for the $[CpW(CO)_2(IMes)]^{+/\bullet}$ and $[CpW(CO)_2(IMes)(MeCN)]^{+/\bullet}$ couples (Table 1) and for the equilibrium constant $K_{MeCN}$ (eq 4) for MeCN dissociation

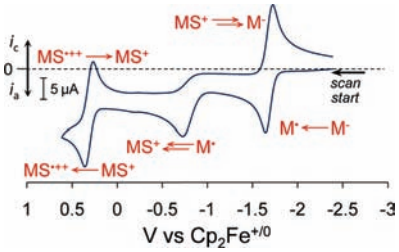


**Figure 1.** Cyclic voltammogram of $[CpW(CO)_2(IMes)]^-[K(18\text{-crown-6})]^+$ in MeCN (0.2 M $^nBu_4N^+PF_6^-$) at 0.1 V s$^{-1}$. M = $CpW(CO)_2(IMes)$; S = MeCN. Multiple arrows indicate combined chemical and electrochemical steps.

**Table 1. $E^\circ$ Values (V vs $Cp_2Fe^{+/0}$) for Redox Processes Observed in the Electrochemical Oxidation of $CpW(CO)_2(IMes)H$ and $[CpW(CO)_2(IMes)]^-[K(18\text{-crown-6})]^+$ in MeCN (0.2 M $^nBu_4N^+PF_6^-$)**

| entry | redox couple | $E^\circ$ |
|---|---|---|
| 1 | $[CpW(CO)_2(IMes)]^{\bullet/-}$ | −1.65(1)[a] |
| 2 | $[CpW(CO)_2(IMes)]^{+/\bullet}$ | −0.49(4)[b] |
| 3 | $[CpW(CO)_2(IMes)(MeCN)]^{+/\bullet}$ | −1.92(8)[b] |
| 4 | $[CpW(CO)_2(IMes)(MeCN)]^{\bullet 2+/+}$ | 0.34(1)[a] |
| 5 | $[CpW(CO)_2(IMes)H]^{\bullet +/0}$ | −0.13(3)[c] |

[a] Reversible couple, recorded at 0.1 V s$^{-1}$ using a 1-mm glassy carbon electrode. [b] Estimated using digital simulation of experimental cyclic voltammograms.[40] [c] Reversible at higher scan rates, recorded at 800 V s$^{-1}$ using a 10-$\mu$m Pt electrode.

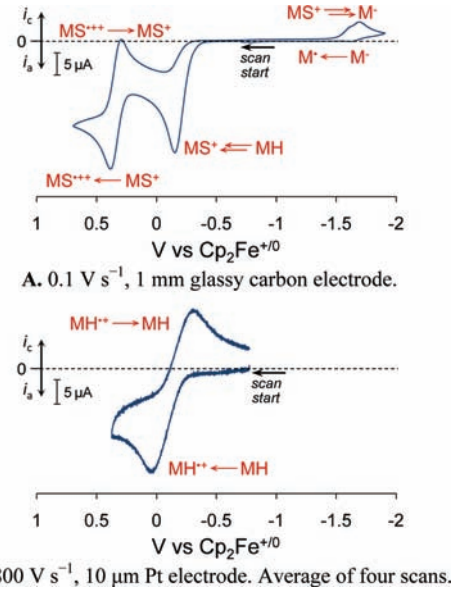


**Figure 2.** Cyclic voltammograms of $CpW(CO)_2(IMes)H$ (MeCN, 0.2 M $^nBu_4N^+PF_6^-$) at the indicated scan rates. M = $CpW(CO)_2(IMes)$; S = MeCN. Multiple arrows indicate coupled chemical and electrochemical steps.

from $[CpW(CO)_2(IMes)(MeCN)]^+$ (5(4) × 10$^{-13}$ M).

$$[CpW(CO)_2(IMes)(MeCN)]^+ \overset{K_{MeCN}}{\rightleftharpoons} [CpW(CO)_2(IMes)]^+ + MeCN \quad (4)$$

These values are employed as inputs to thermochemical cycles for reactions of the neutral hydride, its radical cation, and the cationic dihydride $[CpW(CO)_2(IMes)(H)_2]^+$ as presented below. A detailed treatment of the experimental electrochemistry of $[CpW(CO)_2(IMes)]^-$, $CpW(CO)_2(IMes)^\bullet$, and $[CpW(CO)_2(IMes)(MeCN)]^+$ and the digital simulations mentioned above is reported separately.[40]

**Electrochemical Studies of $CpW(CO)_2(IMes)H$.** Cyclic voltammograms of the neutral hydride $CpW(CO)_2(IMes)H$ show an oxidation wave (Figure 2A) that is irreversible at low scan rates but quasi-reversible at scan rates of 2 V s$^{-1}$ and higher. At a scan rate of 800 V s$^{-1}$ (using a 10-$\mu$m Pt electrode; Figure 2B), the ratio $i_{red}/i_{ox}$ is 0.75, and therefore the average potential of the observed anodic and cathodic peaks is a good estimate of $E^\circ$ for the $[CpW(CO)_2(IMes)H]^{\bullet +/0}$ couple in the absence of following reactions. To minimize the effect of noise, the measurement was repeated four times, producing $E^\circ$ = −0.13 V with a standard deviation of 10 mV. Since the couple is not fully reversible ($i_{red}/i_{ox} < 1$), we assign an uncertainty of 30 mV to this value ($2\sigma$ + 10 mV), reflecting a possible difference in resistance losses ($iR$ drop) for the dissimilar reduction and oxidation waves. The mode of cleavage (homolytic or heterolytic) of the M−H bond in the highly acidic radical cation $[CpW(CO)_2(IMes)H]^{\bullet +}$ formed by oxidation of $CpW(CO)_2(IMes)H$ is discussed in the Supporting Information.

Oxidation of $CpW(CO)_2(IMes)H$ ultimately leads to formation of the solvent adduct $[CpW(CO)_2(IMes)(MeCN)]^+$, as illustrated in Figure 2A. The fully reversible wave at 0.34 V corresponds to the reversible oxidation of $[CpW(CO)_2(IMes)(MeCN)]^+$, producing the 17-electron radical dication $[CpW(CO)_2(IMes)(MeCN)]^{\bullet 2+}$,

which is also observed in voltammograms of $[CpW(CO)_2(IMes)(MeCN)]^+PF_6^-$ and $[CpW(CO)_2(IMes)]^-[K(18\text{-crown-6})]^+$. The complex wave observed between −1.6 and −1.7 V (Figure 2A) corresponds to the ECE reduction converting $[CpW(CO)_2(IMes)(MeCN)]^+$ to $[CpW(CO)_2(IMes)]^-$, as discussed in detail in a separate paper.[40]

**Thermochemical Properties of $CpW(CO)_2(IMes)H$ and Its Derivatives.** Thermochemical cycles[27,41] giving bond strengths for $CpW(CO)_2(IMes)H$, the transient radical cation $[CpW(CO)_2(IMes)H]^{\bullet+}$, and the cationic dihydride $[CpW(CO)_2(IMes)(H)_2]^+$ complexes in MeCN solution ($T$ = 22 °C) have been constructed using the electrochemical and solution equilibrium data presented above. The derived $\Delta G°$ values constitute a comprehensive description of the thermochemistry of $CpW(CO)_2(IMes)H$ and species derived from it by formation or cleavage of W−H and W−NCMe bonds. Scheme 2 presents the free energy relationships between $CpW(CO)_2(IMes)H$ and its derivatives. As this format illustrates, when the values for two sides of a triangle are known, the value for the third side can be calculated. Detailed thermochemical schemes for the cycles shown in Scheme 2 appear in the Supporting Information. All potentials and equilibrium constants have been determined in MeCN as solvent, with the exception of $K_{THF,H_2}$ and $K_{MeCN,H_2}$ (eqs 2 and 3), obtained in THF-$d_8$ as described above. All uncertainties are presented at the 2$\sigma$ confidence level where $\sigma$ has been determined; in cases where it has not, estimates of uncertainty have been assigned. A discussion of our selection of standard states and uncertainties is included in the Supporting Information.

Our notation is illustrated using the following examples: $E°(M^{\bullet/-})$ is the redox potential for the $M^{\bullet}/M^-$ couple, and $pK_a(MH)$ is the acidity of MH in MeCN. $\Delta G°_{H\bullet}(MH)$ is the free energy for the loss of $H^{\bullet}$ from MH, i.e., the dissociation reaction $MH \rightleftharpoons M^{\bullet} + H^{\bullet}$. $\Delta G°_{H^-,S}(MH)$ is the free energy for the displacement of $H^-$ by S, i.e., the substitution reaction $MH + S \rightleftharpoons MS^+ + H^-$.

**Homolytic Cleavage of $H^{\bullet}$ from $CpW(CO)_2(IMes)H$.** The homolytic M−H BDFE of a metal hydride can be determined using a thermochemical cycle that includes deprotonation of MH and oxidation of the $M^-$ anion.[17,19,20,25,27] Scheme 3A presents this thermochemical cycle for $CpW(CO)_2(IMes)H$ (MH), showing the experimentally determined inputs $pK_a(MH)$ and $E°(M^{\bullet/-})$ and the output homolytic W−H BDFE, $\Delta G°_{H\bullet}(MH)$. Scheme 3 also shows how the output of cycle A (shown in bold) is used as an input into cycles B and C for the determination of other free energies, as discussed below.

The redox couple $CpW(CO)_2(IMes)^{\bullet/-}$ is electrochemically reversible at all scan rates employed—an unusual observation since most 17-electron metal-centered radicals rapidly dimerize[20,42]—and thus the $E°$ value (−1.65 V) and the experimentally determined $pK_a$ value for $CpW(CO)_2(IMes)H$ provide a reliable estimate of the homolytic W−H BDFE ($\Delta G°_{H\bullet}(MH)$ = 59.3(3) kcal mol$^{-1}$).

Many prior studies of metal hydride thermochemistry[17,19,20,25,27] reporting bond dissociation enthalpies (BDE values) have been

**Scheme 2. Thermochemical Data for MH (M = $CpW(CO)_2(IMes)$; S = MeCN) and Its Derivatives in MeCN, Showing the Relationships between $E°$ (V vs $Cp_2Fe^{+/0}$), $\Delta G°$ (kcal mol$^{-1}$), and $pK_a^{MeCN}$ Values.**

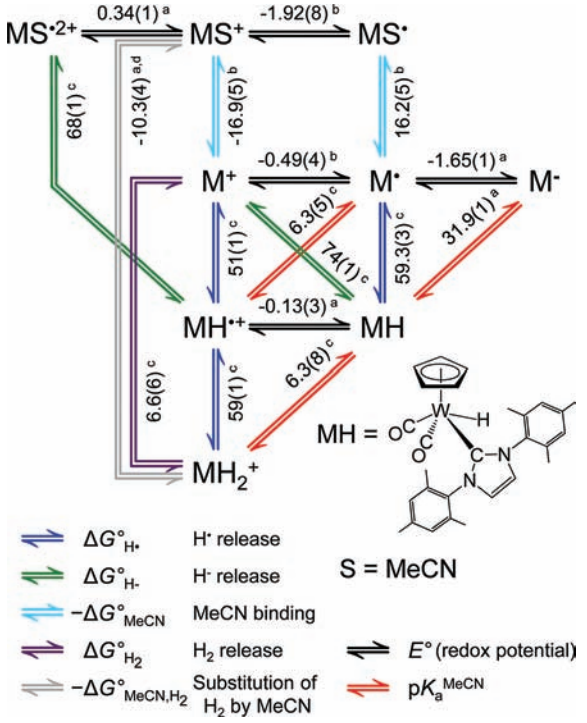


[a] Obtained by direct measurement of reversible redox couples or chemical equilibria. [b] Determined by digital simulation of experimental cyclic voltammograms. [c] Derived using the thermochemical cycles presented in the text. [d] Measured for S = MeCN in THF-$d_8$.

**Scheme 3. Equations for Determination of Thermodynamic Values: (A) $\Delta G°_{H\bullet}(MH)$, (B) $\Delta G°_{H^-}(MH)$, and (C) $\Delta G°_{H^-,S}(MH)$; M = $CpW(CO)_2(IMes)$; S = MeCN**

| | | | | | | $\Delta G°$ (kcal mol$^{-1}$) | |
|---|---|---|---|---|---|---|---|
| A | MH | → $M^- + H^+$ | $\Delta G°_{H^+}(MH)$ | = $1.37pK_a(MH)$ | = | 43.7(1) | |
| | $M^-$ | → $M^{\bullet} + e^-$ | $-\Delta G°(M^{\bullet/-})$ | = $23.06\,E°(M^{\bullet/-})$ | = | −38.0(2) | |
| | $H^+ + e^-$ | → $H^{\bullet}$ | $\Delta G°(H^{+/\bullet})$ [a] | | = | 53.6 | |
| B | **MH** | → $\mathbf{M^{\bullet} + H^{\bullet}}$ | $\mathbf{\Delta G°_{H\bullet}(MH)}$ [b] | | = | **59.3(3)** | (5) |
| | $M^{\bullet}$ | → $M^+ + e^-$ | $-\Delta G°(M^{+/\bullet})$ | = $23.06\,E°(M^{+/\bullet})$ | = | −11.3(9) | |
| | $H^{\bullet} + e^-$ | → $H^-$ | $\Delta G°(H^{\bullet/-})$ [a] | | = | 26.0 | |
| C | **MH** | → $\mathbf{M^+ + H^-}$ | $\mathbf{\Delta G°_{H^-}(MH)}$ [c] | | = | **74(1)** | (6) |
| | $M^+ + S$ | → $MS^+$ | $-\Delta G°_S(MS^+)$ | = $-1.37pK_S(MS^+)$ | = | −16.9(5) | |
| | **MH + S** | → $\mathbf{MS^+ + H^-}$ | $\mathbf{\Delta G°_{H^-,S}(MH)}$ [d] | | = | **57(1)** | (7) |

[a] Determination of $\Delta G°(H^{+/\bullet})$ and $\Delta G°(H^{\bullet/-})$ has been described in detail.[14,41] [b] $\Delta G°_{H\bullet}(MH) = 1.37pK_a(MH) + 23.06E°(M^{\bullet/-}) + 53.6$. See the Supporting Information in ref 14 for a justification of the use of this constant of 53.6 kcal mol$^{-1}$ rather than similar values used by others. [c] $\Delta G°_{H^-}(MH) = 1.37pK_a(MH) + 23.06[E°(M^{\bullet/-}) + E°(M^{+/\bullet})] + 79.6$. [d] $\Delta G°_{H^-,S}(MH) = 1.37[pK_a(MH) - pK_S(MS^+)] + 23.06[E°(M^{\bullet/-}) + E°(M^{+/\bullet})] + 79.6$.

**Table 2. Thermochemical Quantities for $CpW(CO)_2(L)H$ (L = IMes, $PMe_3$, CO) in MeCN**

| L | $pK_a(MH)$ | $E°(M^{\bullet/-})$ (V vs $Cp_2Fe^{+/0}$) | $\Delta G°_{H\bullet}(MH)$ |
|---|---|---|---|
| IMes | 31.9 | −1.65 | 59.3 |
| $PMe_3$ | 26.6[a] | −1.12[c] | 64.2 |
| CO | 16.1[b] | −0.38[c] | 66.9 |

[a] See ref 23. [b] See ref 22. [c] Irreversible oxidations, corrected for potential shifts due to radical dimerization. See ref 20.

determined using eq 8.[26] Comparison of eqs 8 and 9 indicates that BDE values exceed BDFEs, as shown by Wayner and Parker.[41] In cases where BDE values have been reported,[20,26] BDFEs ($\Delta G°_{H\bullet}(MH)$) in Table 2 have been calculated from published $pK_a$ and $E°$ values using the thermochemical cycle shown in Scheme 3A, for comparison with the present results.

$$\mathrm{BDE(MH)} = 1.37pK_a(\mathrm{MH}) + 23.06E°(\mathrm{M}^{\bullet/-}) + 59.5 \quad (8)$$

$$\begin{aligned}\mathrm{BDFE(MH)} &= \Delta G°_{\mathrm{H}\bullet}(\mathrm{MH}) \\ &= \Delta G°_{\mathrm{H}^+}(\mathrm{MH}) - \Delta G°(\mathrm{M}^{\bullet/-}) + \Delta G°(\mathrm{H}^{+/\bullet}) \\ &= 1.37pK_a(\mathrm{MH}) + 23.06E°(\mathrm{M}^{\bullet/-}) + 53.6\end{aligned} \quad (9)$$

**Thermodynamics of $H^-$ Transfer from $CpW(CO)_2(IMes)H$.** Determination of the thermodynamic hydride donor ability of $CpW(CO)_2(IMes)H$ using $pK_a$ and electrochemical data requires the formal potential for oxidation of $CpW(CO)_2(IMes)^\bullet$. However, this oxidation is irreversible (Figure 1) due to the rapid and highly exergonic binding of MeCN to $[CpW(CO)_2(IMes)]^+$, so the required formal potential cannot be determined directly from experimental cyclic voltammograms. This apparent obstacle motivated the digital simulation of voltammograms for the oxidation of $[CpW(CO)_2(IMes)]^-$ and $CpW(CO)_2(IMes)^\bullet$ across a series of different scan rates and analyte concentrations,[40] ultimately providing estimates for $E°(M^{+/\bullet})$ (−0.49(4) V) and $K_{MeCN}$, the equilibrium constant for dissociation of MeCN from $[CpW(CO)_2(IMes)(MeCN)]^+$ (5(4) × $10^{-13}$ $M^{-1}$; eq 4). This value has been converted from the previously reported value[40] to reflect the different standard state definitions used here; see the Supporting Information for a discussion of standard states and uncertainties.

These estimates permit the calculation of the hydride donor ability of $CpW(CO)_2(IMes)H$ in MeCN, both without (Scheme 3B) and with (Scheme 3C) subsequent coordination of MeCN to $[CpW(CO)_2(IMes)]^+$. The 16-electron cation $[CpW(CO)_2(IMes)]^+$ is not directly observed experimentally since it rapidly binds MeCN.

**Thermodynamics of Proton, Hydrogen Atom, and Hydride Transfer from the Radical Cation $[CpW(CO)_2(IMes)H]^{\bullet+}$.** The observed reversibility of oxidation of $CpW(CO)_2(IMes)H$ ($E°$ = −0.13(3) V; Figure 2B) permits the estimation of thermochemical properties of the acidic radical cation $[CpW(CO)_2(IMes)H]^{\bullet+}$, including its acidity ($pK_a(MH^{\bullet+})$ = 6.3(5); Scheme S2, Supporting Information) and the homolytic W−H BDFE, both without and with subsequent MeCN binding ($(\Delta G°_{H\bullet}(MH^{\bullet+})$ = 51(1) kcal $mol^{-1}$, $\Delta G°_{H\bullet,S}(MH^{\bullet+})$ = 34(1) kcal $mol^{-1}$; Schemes S3A and S3B, Supporting Information).

The homolytic M−H BDFE of $[CpW(CO)_2(IMes)H]^{\bullet+}$ may be determined as shown in Scheme S3. As with Scheme 3 above, formation of solvate $MS^+$ following release of $H^\bullet$ from $MH^{\bullet+}$ has a substantial effect on hydrogen atom transfer energetics (A and B in Scheme S3).

Reactivity patterns observed in electrochemical and NMR experiments point to the radical cation $[CpW(CO)_2(IMes)H]^{\bullet+}$ as a reactive intermediate. Dropwise addition of a $CD_3CN$ solution of $CpW(CO)_2(IMes)H$ to a solution of $Cp_2Fe^+PF_6^-$ results in the clean conversion of the hydride to the solvent adduct $[CpW(CO)_2(IMes)(CD_3CN)]^+$ as determined by $^1H$ NMR. According to the Nernst equation, $K_{eq} \approx 150$ ($\Delta E°$ = 130 mV) for electron transfer from $CpW(CO)_2(IMes)H$ to $Cp_2Fe^+$. Electrochemical oxidation of $CpW(CO)_2(IMes)H$ results in the appearance (Figure 1) of a reversible couple at 0.34 V, characteristic of the $[CpW(CO)_2(IMes)(MeCN)]^{\bullet 2+/+}$ redox couple. The chemical or electrochemical oxidation of $CpW(CO)_2(IMes)H$ is thus followed by formal abstraction of $H^\bullet$, but the precise mechanism of cleavage of the W−H bond remains unknown. Various possibilities are considered in the Supporting Information.

Electrochemical oxidation of $[CpW(CO)_2(IMes)(MeCN)]^+$ to give the unusual 17-electron radical dication, $[CpW(CO)_2(IMes)(MeCN)]^{\bullet 2+}$, is cleanly reversible (Figure 2A), allowing the construction of a thermochemical cycle (Scheme S4, Supporting Information) for determination of the hydride donor ability of $[CpW(CO)_2(IMes)H]^{\bullet+}$ in MeCN. The determined hydride donor ability of $[CpW(CO)_2(IMes)H]^{\bullet+}$ includes the solvation of the dicationic product; in this case, unlike $CpW(CO)_2(IMes)H$, the free energy for this solvation is not known, and so the hydride donor ability in the absence of solvent binding cannot be determined. The hydride donor ability of $[CpW(CO)_2(IMes)H]^{\bullet+}$ determined here ($\Delta G°_{H^-,S}(MH^{\bullet+})$ = 68(2) kcal $mol^{-1}$) shows that it is a considerably weaker hydride donor than the neutral hydride ($\Delta G°_{H^-,S}(MH)$ = 57(1) kcal $mol^{-1}$). This is not surprising, since hydride transfer from $[CpW(CO)_2(IMes)H]^{\bullet+}$ gives a dication. The decrease in hydride donor ability of $[CpW(CO)_2(IMes)H]^{\bullet+}$ compared to the neutral hydride $CpW(CO)_2(IMes)H$ accompanies a substantial increase in acidity resulting from oxidation of $CpW(CO)_2(IMes)H$ to $[CpW(CO)_2(IMes)H]^{\bullet+}$.

**Thermochemistry of the Dihydride $[CpW(CO)_2(IMes)(H)_2]^+$: Addition/Elimination of $H_2$ and Release of $H^+$ or $H^\bullet$.** High-pressure NMR methods allowed the direct determination of $K_{S,H_2}(MS^+)$ for S = MeCN in THF-$d_8$ (eq 3). In neat MeCN, the cationic metal complex binds MeCN, and no displacement of MeCN by $H_2$ is observed. Equilibrium displacement values of THF-$d_8$ and MeCN by $H_2$, measured in THF-$d_8$, are taken as estimates for their values in MeCN—these equilibria are between species with charges that do not change, and therefore the difference in solvation energies between $M(H)_2^+$ and $M(MeCN)^+$ is assumed here to be only weakly dependent on whether THF or MeCN is the solvent. This assumption permits estimation of the free energy of $H_2$ release from $[CpW(CO)_2(IMes)(H)_2]^+$ ($\Delta G°_{H_2}(MH_2^+)$ = 6.6(6) kcal $mol^{-1}$; Scheme S5, Supporting Information) and the $pK_a$ value for this species ($pK_a(MH_2^+)$ = 6.3(8); Scheme S6, Supporting Information). This $pK_a$ value is essentially the same as that reported for $[CpW(CO)_2(PMe_3)(H)_2]^+$ ($pK_a$ = 5.6).[15] As with the radical cations, ligand electronic effects appear weaker for deprotonation of these relatively strong acids than for the weak acids $CpW(CO)_2(IMes)H$ and $CpW(CO)_2(PMe_3)H$.

## ■ DISCUSSION

**Homolytic Cleavage of M−H Bonds.** The thermodynamics of homolytic cleavage of metal hydrides are central to the

understanding of hydrogen atom transfer reactions involving metal hydrides.[2] It is difficult to directly observe equilibria where an $H^{\bullet}$ transfer from a metal hydride occurs, because of the very high reactivity of most metal-centered radicals. Consequently, much of the information on homolytic BDEs has come from the use of thermochemical cycles. Breslow showed in 1973 how this could be applied to the determination of the C−H bonds of hydrocarbons,[43] and Bordwell and co-workers used this technique extensively for many organic compounds.[44] Tilset and Parker have used p$K_a$ values for $CpW(CO)_2(L)H$ (L = $PMe_3$, CO) and measured electrochemical potentials for oxidation of the corresponding anions, correcting for kinetic potential shifts associated with the dimerizations of the resultant radicals, to estimate homolytic W−H bond dissociation enthalpies for these species.[20] Their results, along with our own, provide an evaluation of the effects of ligand substitution on W−H homolysis.

The relative contributions of acidity and redox potential to the corresponding homolytic M−H BDFE values for $CpW(CO)_2(L)H$ (L = IMes, $PMe_3$, CO) are shown in Table 2. The value of $E°(M^{\bullet/-})$ shifts toward more reducing potentials with increasing ligand donor ability (IMes > $PMe_3$ > CO), which results in a decrease in the contribution to $\Delta G°_{H^{\bullet}}(MH)$. At the same time, stronger donor ligands lead to increased p$K_a$ values, countering the effect of the trend in $E°(M^{\bullet/-})$. These large but opposing effects result in a moderate decrease in $\Delta G°_{H^{\bullet}}(MH)$ across this series, with $CpW(CO)_2(IMes)H$ having the weakest W−H bond. Extensive studies of M−H BDFEs for late transition metal bis(diphosphine) hydrides[5,7,8,11,14,28,29] have shown that electronic effects have a much greater influence on *heterolytic* M−H BDFEs than on *homolytic* BDFEs. This is expected, because heterolysis results in a change in the charge of the metal species and thus a substantial charge redistribution.[6]

**Hydride Transfer from Metal Hydrides.** Thermodynamic hydride donor abilities for a variety of transition metal hydrides have been determined calorimetrically,[14] by observation of hydride transfer equilibria,[14] and by using thermochemical cycles based on equilibrium heterolysis of $H_2$[5,7,8,11,28,45] or proton transfer from MH followed by two-electron oxidation of $M^-$ (Scheme 3B,C).[14] This last approach is reliable for systems for which the required oxidation potentials can be measured or estimated.

Dissociation of $H^-$ from an 18-electron metal hydride to give a 16-electron metal cation is frequently followed by binding of a two-electron donor (e.g., a solvent molecule such as MeCN) to give an 18-electron product. Methods for determining hydride donor ability inherently include contributions from this coordination step, but the magnitude of the contribution can vary substantially. Hydride transfer from $CpW(CO)_2(IMes)H$ to $Ph_3C^+$ in MeCN leads to the clean formation of $[CpW(CO)_2(IMes)(MeCN)]^+$.[38] Solvated complexes $[CpW(CO)_2(L)(S)]^+$ (L = CO, $PR_3$ , NHC; S = MeCN, THF, ketones, alcohols, etc.) are ubiquitous in the reaction chemistry of $CpW(CO)_2(L)H$ complexes and are known to play an important role as catalytic intermediates.[46] Solvent binding free energies for this class of compounds have thus far been examined by measuring competitive displacement equilibria (e.g., ketones vs alcohols)[35] and thus are relative rather than absolute quantities.

The hydride donor ability of $CpW(CO)_2(IMes)H$ is substantially affected by the binding of MeCN to the 16-electron cation, $[CpW(CO)_2(IMes)]^+$, stabilizing this product by 16.9(5) kcal $mol^{-1}$ through the formation of $[CpW(CO)_2(IMes)(MeCN)]^+$ (Scheme 3C). This indicates that thermodynamic hydricity is *tunable* by selection of solvent in any complex where the 16-electron metal cation binds solvent. McQueen and Hembre have documented that the hydride donor ability of Cp*(dppm)RuH (dppm = 1,2-bis(diphenylphosphino)methane) does indeed vary with solvent, owing to the differences in the strength of MeCN vs THF binding to the metal cation.[47]

For comparison, reversible electrochemical waves have been reported for the oxidation of bis(diphosphine) hydrides of Co, Ir, and Pt and for the first and second oxidations of their conjugate bases.[30,32,34,35] This reversibility suggests that solvent binding and release do not perturb electron transfer equilibria, and solvent effects on $\Delta G°_{H^-}$ for these systems are expected to be lower than for the tungsten complexes studied here. Crystallographic data[5] for $[Co(dppe)_2(MeCN)](PF_6)_2$ (dppe = 1,2-bis(diphenylphosphino)ethane) indicate a weak Co−N interaction.

**Reactivity of Radical Cations of Metal Hydrides.** One-electron oxidation of metal hydrides often has a profound effect on reactivity, activating the M-H bond toward proton transfer and hydrogen atom transfer. The value of $\Delta pK_a$ upon one-electron oxidation of $CpW(CO)_2(IMes)H$ is 25.6, similar to those for $CpCr(CO)_2(L)H$ (L = $PPh_3$, $PEt_3$, $P(OMe)_3$), where $\Delta pK_a$ values of 23.5−25.5 were found.[19] Oxidation of $CpM(CO)_3H$ (M = Cr, Mo, W) or $CpW(CO)_2(PMe_3)H$ decreases the p$K_a$ by a relatively constant 20.6 ± 1.5 units,[25] and a similar change was found for tris(pyrazolyl)borate complexes $Tp(CO)_3MH$ (M = Cr, Mo, W).[17] Thermochemical studies of bis(diphosphine) metal hydride complexes afforded $\Delta pK_a$ = 14.5 for $HCo(dppe)_2$[5] and $\Delta pK_a$ = 18 for $HRh(depx)_2$[6] (depx = α,α′-bis(diethylphosphino)xylene); the p$K_a$ difference between $MH^+$ vs $MH^{\bullet 2+}$ is 20.5 for $[HPt(EtXantphos)_2]^+$ (EtXantphos = 9,9-dimethyl-4,5-bis(diethylphosphino)xanthene).[29]

Comparing the electrochemical data for $CpW(CO)_2(L)H$ and $[CpW(CO)_2(L)]^-$ (L = IMes or $PMe_3$) reveals that $E°(M^{\bullet/-})$ is more sensitive than $E°(MH^{\bullet +/0})$ to the nature of L ($\Delta E$ = 530 vs 290 mV), possibly reflecting differences in $[CpW(CO)_2(L)]^-$ stabilization due to $\pi$ backbonding, which should be stronger for L = $PMe_3$ than IMes.[48] This effect may be less significant for the hydrides than for the anions, as the redox potentials for the anions are more negative.

Thermochemical studies on chromium carbonyl hydrides $CpCr(CO)_2(PR_3)H$ by Tilset[19] found that the homolytic BDE values of these $MH^{\bullet +}$ species are 8−10 kcal $mol^{-1}$ lower than those of the corresponding MH complexes, a significant bond weakening resulting from one-electron oxidation, though one that is much smaller than the degree of activation toward proton transfer in these cases. Several $[HM(diphosphine)_2]^+$ systems (M = Pt, Co, Rh)[5,6,29] show a decrease in homolytic M−H BDFE values due to one-electron oxidation, with known examples ranging from 9 to 24 kcal $mol^{-1}$. Oxidation of closed-shell $[HCo(dppe)_2]^+$ to open-shell $[HCo(dppe)_2]^{2+}$ lowers the homolytic Co−H BDFE by 9 kcal $mol^{-1}$, while further oxidation of open-shell $[HCo(dppe)_2]^{2+}$ to closed-shell $[HCo(dppe)_2]^{3+}$ *raises* the homolytic Co−H BDFE by 3 kcal $mol^{-1}$. Similarly, data from $Cp^*_2Mo_2S_3(SH)$, $Cp^*_2Mo_2S_2(SH)_2$, and $Cp^*_2Mo_2S_2(SMe)(SH)$ complexes uniformly show a weakening of the S−H bonds of 9−24 kcal $mol^{-1}$ as a result of oxidation *or* reduction reactions converting closed-shell species to open-shell species.[12] In contrast, Poli reported an example in which one-electron oxidation of $Cp^*(dppe)WH_3$ led to a W−H bond that was stronger in the radical cation than in the neutral hydride,[49] according to infrared spectroscopy and DFT computations.

**Reactivity of the Dihydride Complex.** Dihydrides $[CpM(CO)_2(L)(H)_2]^+$ (M = Mo, W; L = IMes, $PR_3$) are invoked as reactive intermediates in the catalytic ionic hydrogenation of ketones, with proton transfer from the cationic dihydride to the ketone producing the neutral hydride, followed by hydride transfer from the neutral hydride.[46,50] The $pK_a$ of protonated acetone in MeCN is about −0.1,[18,51] so it is clear that the proton transfer from either $[CpW(CO)_2(IMes)(H)_2]^+$ or $[CpW(CO)_2(PMe_3)(H)_2]^+$ to a ketone is substantially endergonic. This helps explain why they are not very active catalysts for ketone hydrogenation, even though subsequent hydride transfer from the neutral hydride to the protonated ketone is exergonic.

The value of $pK_a^{MeCN}$ for $[CpW(CO)_2(IMes)(H)_2]^+$ (6.3(8)) is essentially the same as that obtained above for the radical cation $[CpW(CO)_2(IMes)H]^{\bullet+}$ (6.3(5)). The similarity of these two $pK_a$ values points to an interesting feature of metal hydride systems: in cases where the $pK_a$ values of a *cationic dihydride* and the corresponding *cationic radical monohydride* are similar, the homolytic BDFE values of the *cationic dihydride* and the *neutral hydride* must also be similar. This is illustrated in Scheme 2, in the parallelogram defined by $MH_2^+$, $MH^{\bullet+}$, MH, and $M^\bullet$: the two routes connecting $MH_2^+$ and $M^\bullet$ both consist of a proton transfer and a hydrogen atom transfer; $[CpW(CO)_2(IMes)(H)_2]^+$ and $[CpW(CO)_2(IMes)H]^{\bullet+}$ have similar $pK_a$ values, and the homolytic W−H BDFE values of $[CpW(CO)_2(IMes)(H)_2]^+$ and $CpW(CO)_2(IMes)H$ are also similar: $\Delta G^\circ_{H^\bullet}(MH_2^+)$ = 59(1) kcal mol$^{-1}$ (Scheme S7, Supporting Information) and $\Delta G^\circ_{H^\bullet}(MH)$ = 59.3(5) kcal mol$^{-1}$ (Scheme 3A). Literature data may be used to estimate the homolytic W−H BDFE of the cationic dihydride $CpW(CO)_2(PMe_3)(H)_2^+$ at ∼65 kcal mol$^{-1}$,[15,25] again essentially the same as the value of 64.2 kcal mol$^{-1}$ for $CpW(CO)_2(PMe_3)H$ (determined using Scheme 3A with reported data and Scheme S7).[20]

This relationship appears to hold for a variety of different transition metal hydride systems, with homolytic M−H BDFEs of dihydrides being about 1 kcal mol$^{-1}$ lower than those of their corresponding monohydrides. The homolytic M−H BDFEs are nearly equal for $HCo(dppe)_2$ (59.1 kcal mol$^{-1}$) and the corresponding dihydride $[(H)_2Co(dppe)_2]^+$ (58.0 kcal mol$^{-1}$);[5] related Pt complexes[29] also show very similar BDFEs for the hydride $[HPt(EtXantphos)_2]^+$ (69 kcal mol$^{-1}$) and the dihydride $[(H)_2Pt(EtXantphos)_2]^{2+}$ (68 kcal mol$^{-1}$); the neutral Rh complex $HRh(depx)_2$ (70 kcal mol$^{-1}$) and the cationic dihydride $[(H)_2Rh(depx)_2]^+$ (67 kcal mol$^{-1}$) show the same trend.[6] In these cases, due to the "parallelogram" relation described above, the $pK_a$ values of these dihydrides will be similar to the $pK_a$ values of the corresponding monohydrides having the same charge.

## CONCLUSIONS

Systematic determination of the free energy changes associated with binding or release of $H^+$, $H^\bullet$, $H^-$, and $H_2$ in metal hydride systems has provided a quantitative basis for understanding the factors influencing their bond dissociation energies for homolytic and heterolytic processes. This study of the metal hydride $CpW(CO)_2(IMes)H$, the radical cation $[CpW(CO)_2(IMes)H]^{\bullet+}$, and the dihydride $[CpW(CO)_2(IMes)(H)_2]^+$ provides insights into the substantial effects of *N*-heterocyclic carbene ligands on homolytic and heterolytic bond free energies. The large difference in acidity of $CpW(CO)_2(IMes)H$ ($pK_a$ = 31.9) vs $CpW(CO)_2(PMe_3)H$ ($pK_a$ = 26.6) shows that IMes is a very powerful electron-donating ligand, greatly exceeding the donor strength of $PMe_3$. Additionally, this study provides a quantitative understanding of solvent effect upon hydride donor ability: binding of MeCN to the 16-electron cationic product, $[CpW(CO)_2(IMes)]^+$ (−16.9 kcal mol$^{-1}$), has a large effect on the hydride donor ability of $CpW(CO)_2(IMes)H$. Thermodynamic hydricity is thus tunable by choice of solvent in any metal hydride that binds solvent after hydride transfer.

These results provide evidence that, in both $CpW(CO)_2(IMes)H$ and $CpW(CO)_2(PMe_3)H$, the homolytic M−H BDFEs for the neutral hydrides are essentially identical to those of the corresponding cationic dihydrides. This finding is tantalizing evidence that the trend may be general, since it has also been observed for late transition metal carbonyls and bis(diphosphine) adducts.[5,6,29] These studies underscore the value of thermochemical characterization in the development of a better understanding of the reactivity of metal hydrides in stoichiometric and catalytic reactions.

## EXPERIMENTAL SECTION

**General.** All manipulations were carried out under $N_2$ using standard vacuum line, Schlenk, and inert-atmosphere glovebox techniques. MeCN (Alfa-Aesar, anhydrous amine-free), hexanes (Fisher GC Resolv), and diethyl ether (Burdick and Jackson, anhydrous, nonstabilized) were purified by passage through neutral alumina, and methanol (J. T. Baker, anhydrous) was purified by passage through calcium sulfate, using an Innovative Technology, Inc. PureSolv solvent purification system. Deuterated solvents (Cambridge Isotope Laboratories, 99.5% D or greater) were dried as follows: tetrahydrofuran-$d_8$ was vacuum transferred from sodium−potassium alloy; $CD_3CN$ was stirred for 1 week over $P_2O_5$ and then vacuum distilled through a glass wool plug. $^nBu_4N^+PF_6^-$ (Aldrich) was recrystallized from methanol−ether and dried *in vacuo* at 150 °C for 16 h prior to use. Bibenzyl (Aldrich) was recrystallized from cold hexanes. *p*-Anisidine (Aldrich), tetrafluoroboric acid (Alfa-Aesar, 50−54% w/v in ether), 2,8,9-trimethyl-2,5,8,9-tetraaza-1-phosphabicyclo[3.3.3]undecane (methyl version of Verkade's superbase (VSB), Aldrich), ferrocene (Aldrich), decamethylferrocene (Aldrich), and $Cp_2Co^+PF_6^-$ (Cole-Parmer) were used as received. *p*-Anisidinium tetrafluoroborate was isolated by adding excess $HBF_4\cdot OEt_2$ to an ether solution of *p*-anisidine, isolating the precipitate by filtration, and rinsing with ether. The protonated form of VSB, $[(VSB)H]^+BF_4^-$, was isolated by reacting *p*-anisidinium tetrafluoroborate with excess VSB in MeCN, evaporating the solvent, and extracting with diethyl ether to afford a white, crystalline precipitate that had $^1$H NMR chemical shifts matching literature values.[52] $CpW(CO)_2(IMes)H$,[34,35] $[CpW(CO)_2(IMes)]^+B(C_6F_5)_4^-$,[34,35] $[CpW(CO)_2(IMes)]^-[K(18\text{-crown-}6)]^+$,[38] and $[CpW(CO)_2(IMes)]^+B(C_6F_5)_4^-$[38] were prepared as reported.

**Electrochemical Measurements.** Electrochemical measurements were performed using a CH Instruments 660C potentiostat equipped with a standard three-electrode cell, which was assembled and used within a glovebox. The working electrode was either a 1 mm glassy carbon disk encased in PEEK (Cypress Systems EE040) or a 10 $\mu$m platinum disk encased in glass (Cypress Systems EE016) and was polished before each run using alumina (BAS CF-1050, dried at 150 °C under vacuum) suspended in MeCN, and then rinsed with neat MeCN. A glassy carbon rod (Structure Probe, Inc.) was used as the counter electrode, and a silver wire suspended in a solution of $^nBu_4N^+PF_6^-$ (0.2 mM) in MeCN and separated from the analyte solution by a Vycor frit (CH Instruments 112) was used a pseudoreference electrode. All potentials are reported vs the $Cp_2Fe^{+/0}$ couple and were determined relative to an internal reference: $Cp_2Fe^{+/0}$; $(C_5Me_5)_2Fe^{+/0}$, $E^\circ$ = −0.50 V; or $Cp_2Co^{+/0}$, $E^\circ$ = −1.33 V. Unless otherwise noted, measurements were carried out in MeCN (0.2 M $^nBu_4N^+PF_6^-$) at a scan rate of 0.1 V s$^{-1}$.

Estimated standard deviation ($\sigma$) values for $E°$ of reversible couples are assumed to be 0.01 V, the same as the standard deviation of four measurements of $E°$ for the internal reference measured under under the same experimental conditions.

**Determination of the p$K_a^{MeCN}$ of CpW(CO)$_2$(IMes)H.** All spectra were acquired by a single transient without preacquisition pulses. Relative integral values were observed to stabilize within 6 h, and each sample was allowed to stand for 24 h before data used for p$K_a$ determination were collected. Two independent samples of CpW(CO)$_2$(IMes)H in MeCN-$d_3$ (with bibenzyl as an internal standard) along with VSB, and one sample containing [CpW(CO)$_2$(IMes)]$^-$[K(18-crown-6)]$^+$ together with [(VSB)H]$^+$BF$_4^-$, were prepared. Equilibrium concentrations were determined by integrating the Cp resonances of CpW(CO)$_2$(IMes)H and [CpW(CO)$_2$(IMes)]$^-$[K(18-crown-6)]$^+$, the methylene proton signals from the base and its conjugate acid, and the bibenzyl methylene resonance. Results from each sample all gave a p$K_a$ value for CpW(CO)$_2$(IMes)H in MeCN of 31.9, using a p$K_a$ value of 32.90 for [(VSB)H]$^+$.[37]

**High-Pressure NMR Measurements.** ***Caution!*** These experiments must be conducted using appropriate safety measures, including but not limited to blast shields, burst discs, and appropriately rated high-pressure equipment. For a series of $H_2$ displacement equilibrium measurements, sample solutions were exposed to $H_2$ gas pressures from 4.5 to 134 atm throughout equilibration and acquisition phases. These experiments employed a custom-fabricated polyether ether ketone (PEEK) sample cell assembly[39,53] interfaced with a high-pressure gas manifold. Sample cell designs and a configuration for the high-pressure manifold, along with important safety considerations, have been previously reported.[39,53] The entire sample cell assembly was charged with sample solution under anhydrous, anaerobic conditions. For experiments wherein THF-$d_8$ was used as solvent, a 2.5-mm OD spectrophotometric grade glass tube (Wilmad) sealed at one end was introduced into the PEEK NMR tube to serve as a liner, mitigating solvent-induced weakening of the PEEK polymer and improving line shapes.

Equilibrium constants $K_{THF,H_2}$ (eq 2) and $K_{MeCN,H_2}$ (eq 3) were determined as follows: In a glovebox, the PEEK NMR sample tube was charged with a solution containing 10−20 mg of analyte, [CpW(CO)$_2$(IMes)]$^+$B(C$_6$F$_5$)$_4^-$ or [CpW(CO)$_2$(IMes)(MeCN)]$^+$B(C$_6$F$_5$)$_4^-$, in the desired solvent (containing 11.5 mM bibenzyl as an internal standard for integration). The cell was assembled and connected to a high-pressure manifold. Before the sample solution was exposed to manifold gases, the manifold was pressurized to 70 atm $H_2$ and depressurized to 3 atm three times. The NMR probe was tuned, and an initial spectrum was acquired. The tube was removed from the probe and mounted into a mechanical vortex mixer to facilitate equilibration between the gas and liquid phases at the desired $H_2$ pressure. The sample was equilibrated for at least 1 h while vortexing, and spectra were periodically acquired until integral values for selected peaks were observed to stabilize. Once stable chemical equilibria were apparent, data were collected using 128 transients with a delay of 1 s. After data acquisition, the sample was re-equilibrated at the next $H_2$ pressure with vortex mixing. Measurements were collected at three different $H_2$ pressures, approaching equilibrium from both reactant and product sides of the equation, for determination of $K_{THF,H_2}$ (eq 2). The sample tube was carefully vented under vortexing after the experiments were complete.

**Determination of $K_{THF,H_2}$.** [CpW(CO)$_2$(IMes)]$^+$B(C$_6$F$_5$)$_4^-$ was converted quantitatively to [CpW(CO)$_2$(IMes)(THF-$d_8$)]$^+$B(C$_6$F$_5$)$_4^-$ when dissolved in THF-$d_8$. Introduction of $H_2$ to this solution resulted in the formation of [CpW(CO)$_2$(IMes)(H)$_2$]$^+$B(C$_6$F$_5$)$_4^-$.[35] Integrals for the partially overlapping Cp resonances of [CpW(CO)$_2$(IMes)(THF-$d_8$)]$^+$ and [CpW(CO)$_2$(IMes)(H)$_2$]$^+$ ($\delta$ 5.31, fwhm = 3.5 and $\delta$ 5.34, fwhm = 3.8 Hz, respectively) were estimated by simulation using gNMR.[54] Integrals for the free $H_2$ resonance were corrected for a 25% abundance of NMR-silent *para*-$H_2$. Data collected with $P_{H_2}$ = 3.4, 6.8, and 3.4 atm, in that order, gave $K_{THF,H_2}$ = 0.5(3) atm$^{-1}$. Our previously reported value[35] of $K'_{THF,H_2} = 3 \times 10^3$, expressed with [$H_2$] = 1 M and [THF-$d_8$] = 1 M taken as the standard states, is equivalent to $K'_{THF,H_2}$ = 0.5 atm$^{-1}$ using the present standard state definitions (1 atm $H_2$, neat solvent), in agreement with the results reported here. Interconversion between different standard state definitions is presented in the Supporting Information.

**Determination of $K_{MeCN,H_2}$ in THF-$d_8$.** For the measurement of solvent displacement by $H_2$ the B(C$_6$F$_5$)$_4^-$ salt was used rather than the PF$_6^-$ salt of the [CpW(CO)$_2$(IMes)(MeCN)]$^+$ cation in order to avoid complications arising from ion-pairing.[38] When [CpW(CO)$_2$(IMes)(MeCN)]$^+$B(C$_6$F$_5$)$_4^-$ was dissolved in THF-$d_8$, both [CpW(CO)$_2$(IMes)(MeCN)]$^+$ and trace amounts (less than 1%) of [CpW(CO)$_2$(IMes)(THF-$d_8$)]$^+$ were observed along with free MeCN. At elevated $H_2$ pressures, measurable amounts of [CpW(CO)$_2$(IMes)(H)$_2$]$^+$ were also observed: at $P_{H_2}$ = 170 atm ([$H_2$] = 340 mM), 11% of the [CpW(CO)$_2$(IMes)(MeCN)]$^+$ was converted to [CpW(CO)$_2$(IMes)(H)$_2$]$^+$. Integration of spectra collected at $P_{H_2}$ = 34, 170, and 136 atm (in that order) establishes $K_{MeCN,H_2} = 3(2) \times 10^{-8}$ atm$^{-1}$ ($\Delta G° = 10.3(3)$ kcal mol$^{-1}$; eq 3). The diagnostic dihydride resonance of [CpW(CO)$_2$(IMes)(H)$_2$]$^+$ at −0.74 ppm is also evident in these spectra. Line shape analysis failed to converge in this case, likely due to the fact that the Cp integrals of [CpW(CO)$_2$(IMes)(H)$_2$]$^+$ and [CpW(CO)$_2$(IMes)(THF-$d_8$)]$^+$ were small compared to the Cp integral of [CpW(CO)$_2$(IMes)(MeCN)]$^+$. The analysis instead used directly measured integrals, including one integral spanning the partially overlapping Cp resonances of [CpW(CO)$_2$(IMes)(H)$_2$]$^+$ and [CpW(CO)$_2$(IMes)(THF-$d_8$)]$^+$. The absolute concentrations of these minor constituents were determined using this combined integral, along with the $H_2$ integral, the bibenzyl integration standard, and the value of $K_{THF,H_2}$ determined as described above. The concentration of free MeCN was then determined, and the value of $K_{MeCN,H_2}$ was calculated from these concentrations according to eq 3 above.

## ■ ASSOCIATED CONTENT

**Supporting Information.** Cyclic voltammogram showing the oxidation of our selection of standard states; interconversion between different standard state definitions; mechanisms for the oxidation of CpW(CO)$_2$(IMes)H to produce [CpW(CO)$_2$(IMes)(MeCN)]$^+$; thermochemical cycles for the determination of all free energy changes shown in Scheme 2. This material is available free of charge via the Internet at http://pubs.acs.org.

## ■ AUTHOR INFORMATION

**Corresponding Author**
morris.bullock@pnnl.gov

## ■ ACKNOWLEDGMENT

This paper is dedicated to the memory of Jim Franz (1948−2010). We thank the U.S. Department of Energy, Office of Science, Office of Basic Energy Sciences, Division of Chemical Sciences, Biosciences and Geosciences for support of this work. Pacific Northwest National Laboratory is operated by Battelle for the U.S. Department of Energy. We thank Dr. Edwin van der Eide for many helpful discussions, and Dr. John Linehan for assistance with the high-pressure NMR experiments.

## ■ REFERENCES

(1) For a review of proton transfer reactions of metal hydrides, see: Kristjánsdóttir, S. S.; Norton, J. R. Acidity of Hydrido Transition Metal Complexes in Solution. In *Transition Metal Hydrides*; Dedieu, A., Ed.; VCH: New York, 1991; Chapter 9, pp 309−359.

(2) For a review of hydrogen atom transfer reactions of metal hydrides, see: Eisenberg, D. C.; Norton, J. R. *Isr. J. Chem.* **1991**, *31*, 55–66.
(3) For a review of hydride transfer reactions of metal hydrides, see: Labinger, J. A. Nucleophilic Reactions of Metal Hydrides. In *Transition Metal Hydrides*; Dedieu, A., Ed.; VCH: New York, 1991; Chapter 10, pp 361−379.
(4) (a) Rakowski DuBois, M.; DuBois, D. L. *Acc. Chem. Res.* **2009**, *42*, 1974–1982. (b) Rakowski DuBois, M.; DuBois, D. L. *Chem. Soc. Rev.* **2009**, *38*, 62–72. (c) Rakowski DuBois, M.; DuBois, D. L. In *Catalysis Without Precious Metals*; Bullock, R. M., Ed.; Wiley-VCH: Weinheim, 2010. (d) DuBois, D. L.; Bullock, R. M. *Eur. J. Inorg. Chem.* **2011**, 1017–1027.
(5) Ciancanelli, R.; Noll, B. C.; DuBois, D. L.; Rakowski DuBois, M. *J. Am. Chem. Soc.* **2002**, 2984–2992.
(6) Raebiger, J. W.; DuBois, D. L. *Organometallics* **2005**, *24*, 110–118.
(7) Berning, D. E.; Noll, B. C.; DuBois, D. L. *J. Am. Chem. Soc.* **1999**, *121*, 11432–11447.
(8) Berning, D. E.; Miedaner, A.; Curtis, C. J.; Noll, B. C.; Rakowski DuBois, M. C.; DuBois, D. L. *Organometallics* **2001**, *20*, 1832–1839.
(9) Fraze, K.; Wilson, A. D.; Appel, A. M.; Rakowski DuBois, M.; DuBois, D. L. *Organometallics* **2007**, *26*, 3918–3924.
(10) Aresta, M.; Dibenedetto, A.; Pápai, I.; Schubert, G.; Macchioni, A.; Zuccaccia, D. *Chem.—Eur. J.* **2004**, *10*, 3708–3716.
(11) Raebiger, J. W.; Miedaner, A.; Curtis, C. J.; Miller, S. M.; Anderson, O. P.; DuBois, D. L. *J. Am. Chem. Soc.* **2004**, *126*, 5502–5514.
(12) Appel, A. M.; Lee, S.-J.; Franz, J. A.; DuBois, D. L.; Rakowski DuBois, M. *J. Am. Chem. Soc.* **2009**, *131*, 5224–5232.
(13) Appel, A. M.; Lee, S.-J.; Franz, J. A.; DuBois, D. L.; Rakowski DuBois, M.; Twamley, B. *Organometallics* **2009**, *28*, 749–754.
(14) Ellis, W. W.; Raebiger, J. W.; Curtis, C. J.; Bruno, J. W.; DuBois, D. L. *J. Am. Chem. Soc.* **2004**, *126*, 2738–2743.
(15) Papish, E. T.; Rix, F. C.; Spetseris, N.; Norton, J. R.; Williams, R. D. *J. Am. Chem. Soc.* **2000**, *122*, 12235–12242.
(16) (a) Tang, L.; Papish, E. T.; Abramo, G. P.; Norton, J. R.; Baik, M.-H.; Friesner, R. A.; Rappé, A. *J. Am. Chem. Soc.* **2003**, *125*, 10093–10102. (b) Tilset, M. *Inorg. Chem.* **1994**, *33*, 3121–3126.
(17) Skagestad, V.; Tilset, M. *J. Am. Chem. Soc.* **1993**, *115*, 5077–5083.
(18) Smith, K.-T.; Norton, J. R.; Tilset, M. *Organometallics* **1996**, *15*, 4515–4520.
(19) Tilset, M. *J. Am. Chem. Soc.* **1992**, *114*, 2740–2741.
(20) Tilset, M.; Parker, V. D. *J. Am. Chem. Soc.* **1989**, *111*, 6711–6717. *J. Am. Chem. Soc.* **1990**, *112*, 2843.
(21) Tolman, C. A. *Chem. Rev.* **1977**, *77*, 313–348.
(22) Jordan, R. F.; Norton, J. R. *J. Am. Chem. Soc.* **1982**, *104*, 1255–1263.
(23) Moore, E. J.; Sullivan, J. M.; Norton, J. R. *J. Am. Chem. Soc.* **1986**, *108*, 2257–2263.
(24) Kristjánsdóttir, S. S.; Moody, A. E.; Weberg, R. T.; Norton, J. R. *Organometallics* **1988**, *7*, 1983–1987.
(25) Ryan, O. B.; Tilset, M.; Parker, V. D. *J. Am. Chem. Soc.* **1990**, *112*, 2618–2626.
(26) Parker, V. D.; Handoo, K. L.; Roness, F.; Tilset, M. *J. Am. Chem. Soc.* **1991**, *113*, 7493–7498.
(27) Tilset, M. Organometallic Electrochemistry: Thermodynamics of Metal-Ligand Bonding. In *Comprehensive Organometallic Chemistry III*; Crabtree, R. H., Mingos, D. M. P., Eds.; Elsevier: Amsterdam, 2007.
(28) (a) Curtis, C. J.; Miedaner, A.; Ellis, W. W.; DuBois, D. L. *J. Am. Chem. Soc.* **2002**, *124*, 1918–1925. (b) Ellis, W. W.; Ciancanelli, R.; Miller, S. M.; Raebiger, J. W.; Rakowski DuBois, M.; DuBois, D. L. *J. Am. Chem. Soc.* **2003**, *125*, 12230–12236.
(29) Miedaner, A.; Raebiger, J. W.; Curtis, C. J.; Miller, S. M.; DuBois, D. L. *Organometallics* **2004**, *23*, 2670–2679.
(30) (a) Dröge, T.; Glorius, F. *Angew. Chem., Int. Ed.* **2010**, *49*, 6490–6952. (b) Díez-González, S.; Marion, N.; Nolan, S. P. *Chem. Rev.* **2009**, *109*, 3612–3676. (c) Herrmann, W. A. *Angew. Chem., Int. Ed.* **2002**, *41*, 1290–1309. (d) Bourissou, D.; Guerret, O.; Gabbaï, F. P.; Bertrand, G. *Chem. Rev.* **2000**, *100*, 39–91. (e) Herrmann, W. A.; Köcher, C. *Angew. Chem., Int. Ed. Engl.* **1997**, *36*, 2162–2187.
(31) (a) Díez-González, S.; Nolan, S. P. *Coord. Chem. Rev.* **2007**, 874–883. (b) Scott, N. M.; Clavier, H.; Mahjoor, P.; Stevens, E. D.; Nolan, S. P. *Organometallics* **2008**, *27*, 3181–3186. (c) Kelly, R. A., III; Clavier, H.; Giudice, S.; Scott, N. M.; Stevens, E. D.; Bordner, J.; Samardjiev, I.; Hoff, C. D.; Cavallo, L.; Nolan, S. P. *Organometallics* **2008**, *27*, 202–210. (d) Dorta, R.; Stevens, E. D.; Scott, N. M.; Costabile, C.; Cavallo, L.; Hoff, C. D.; Nolan, S. P. *J. Am. Chem. Soc.* **2005**, *127*, 2485–2495. (e) Huang, J.; Schanz, H.-J.; Stevens, E. D.; Nolan, S. P. *Organometallics* **1999**, *18*, 2370–2375. (f) Huang, J.; Jafarpour, L.; Hillier, A. C.; Stevens, E. D.; Nolan, S. P. *Organometallics* **2001**, *20*, 2878–2882.
(32) Gusev, D. G. *Organometallics* **2009**, *28*, 6458–6461.
(33) Zhu, Y.; Fan, Y.; Burgess, K. *J. Am. Chem. Soc.* **2010**, *132*, 6249–6253.
(34) Dioumaev, V. K.; Szalda, D. J.; Hanson, J.; Franz, J. A.; Bullock, R. M. *Chem. Commun.* **2003**, 1670–1671.
(35) Wu, F.; Dioumaev, V. K.; Szalda, D. J.; Hanson, J.; Bullock, R. M. *Organometallics* **2007**, *26*, 5079–5090.
(36) Tang, J.; Dopke, J.; Verkade, J. K. *J. Am. Chem. Soc.* **1993**, *115*, 5015–5020. Verkade, J. G. *Acc. Chem. Res.* **1993**, *26*, 483–489.
(37) Kisanga, P. B.; Verkade, J. G.; Schwesinger, R. *J. Org. Chem.* **2000**, *65*, 5431–5432.
(38) Roberts, J. A. S.; Franz, J. A.; van der Eide, E. F.; Walter, E. D.; Petersen, J. L.; DuBois, D. L.; Bullock, R. M. *J. Am. Chem. Soc.* **2011**, *133*, No. http://dx.doi.org/10.1021/ja202754e (preceding paper in this issue).
(39) Yonker, C. R.; Linehan, J. C. *J. Organomet. Chem.* **2002**, *650*, 249–257. (b) Shaw, W. J.; Linehan, J. C.; Szymczak, N. K.; Heldebrant, D. J.; Yonker, C.; Camaioni, D. M.; Baker, R. T.; Autrey, T. *Angew. Chem., Int. Ed.* **2008**, *47*, 7493–7496.
(40) Roberts, J. A. S.; DuBois, D. L.; Bullock, R. M. *Organometallics* ASAP, August 8, 2011 (http://dx.doi.org/10.1021/om2002816)
(41) Wayner, D. D. M.; Parker, V. D. *Acc. Chem. Res.* **1993**, *26*, 287–294.
(42) Meyer, T. J.; Caspar, J. V. *Chem. Rev.* **1985**, *85*, 187–218.
(43) Breslow, R.; Chu, W. *J. Am. Chem. Soc.* **1973**, *95*, 411–418.
(44) Bordwell, F. G.; Zhang, X. M. *Acc. Chem. Res.* **1993**, *26*, 510–517.
(45) Price, A. J.; Ciancanelli, R.; Noll, B. C.; Curtis, C. J.; DuBois, D. L.; DuBois, M. R. *Organometallics* **2002**, *21*, 4833–4839.
(46) (a) Bullock, R. M.; Voges, M. H. *J. Am. Chem. Soc.* **2000**, *122*, 12594–12595. (b) Voges, M. H.; Bullock, R. M. *J. Chem. Soc., Dalton Trans.* **2002**, 759–770. (c) Song, J.-S.; Szalda, D. J.; Bullock, R. M. *Organometallics* **2001**, *20*, 3337–3346.
(47) McQueen, J. S. Hydrogenase Enzyme Reactivity Modeling with Transition-Metal Hydride and Dihydrogen Complexes. Ph.D. Thesis, University of Nebraska, 1995.
(48) (a) Jacobsen, H.; Correa, A.; Poater, A.; Costabile, C.; Cavallo, L. *Coord. Chem. Rev.* **2009**, *253*, 687–703. (b) Tafipolsky, M.; Scherer, W.; Öfele, K.; Artus, G.; Pedersen, B.; Herrmann, W. A.; McGrady, G. S. *J. Am. Chem. Soc.* **2002**, *124*, 5865–5880. (c) Jacobsen, H.; Correa, A.; Costabile, C.; Cavallo, L. *J. Organomet. Chem.* **2006**, *691*, 4350–4358. (d) Baba, E.; Cundari, T. R.; Firkin, I. *Inorg. Chim. Acta* **2005**, *358*, 2867–2875. (e) Tonner, R.; Heydenrych, G.; Frenking, G. *Chem.—Asian J.* **2007**, *2*, 1555–1567.
(49) (a) Pleune, B.; Poli, R.; Fettinger, J. C. *J. Am. Chem. Soc.* **1998**, *120*, 3257–3258. (b) Pleune, B.; Morales, D.; Meunier-Prest, R.; Richard, P.; Collange, E.; Fettinger, J. C.; Poli, R. *J. Am. Chem. Soc.* **1999**, *121*, 2209–2225.
(50) (a) Bullock, R. M. *Chem.—Eur. J.* **2004**, *10*, 2366–2374. (b) Bullock, R. M. Ionic Hydrogenations. In *Handbook of Homogeneous Hydrogenation*; de Vries, J. G., Elsevier, C. J., Eds.; Wiley-VCH: Weinheim, Germany, 2007; Vol. 1, Chapter 7, pp 153−197. (c) Bullock, R. M. In *Catalysis Without Precious Metals*; Bullock, R. M., Ed.; Wiley-VCH: Weinheim, 2010.

(51) Kolthoff, I. M.; Chantooni, M. K., Jr. *J. Am. Chem. Soc.* **1973**, *95*, 8539–8546.
(52) Lensink, C.; Xi, S. K.; Daniels, L. M.; Verkade, J. G. *J. Am. Chem. Soc.* **1989**, *111*, 3478–3479.
(53) Wallen, S. L.; Schoenbachler, L. K.; Dawson, E. D.; Blatchford, M. A. *Anal. Chem.* **2000**, *72*, 4230–4234.
(54) Budzelaar, P. H. M. *gNMR*, v. 5.0.6.0; IvorySoft, 2006.